

# Experimental and Theoretical Results for Weak Charge Current Backward Proton Production

C. E. Carlson

*Physics Department, College of William and Mary, Williamsburg, VA 23187, USA*

J. Hanlon

*Fermi National Accelerator Laboratory, Batavia, IL, 60510*

K. E. Lassila

*Department of Physics and Astronomy, Iowa State University, Ames, IA 50011*

(February 1999)

In this paper, we do three things in the study of deuteron break-up by high energy neutrino beams. (1) We present previously unpublished data on neutrino induced backward protons from deuteron targets; (2) we calculate the contributions from both the two-nucleon (2N) and six-quark (6q) deuteron components, which depend upon the overall normalization of the part that is 6q; and (3) we suggest other signatures for distinguishing the 2N and 6q clusters. We conclude that the 6q cluster easily explains the shape of the high momentum backward proton spectrum, and its size is nicely explained if the amount of 6q is one or a few percent by normalization of the deuteron. There is a crossover, above which the 6q contribution is important or dominant, at 300–400 MeV/c backward proton momentum.

## I. INTRODUCTION

It is worthwhile to examine and probe the deuteron as a target from many viewpoints because of the role it plays as our main source of information on the neutron. This has become of increasing interest in recent years with unexpected results being found for the numerous sum rules in which neutron structure functions enter. These include the results for the Ellis-Jaffe sum rules [1,2], for the Gottfried sum rule [3], and for the Bjorken sum rule [4,5], prompting us to re-examine assumptions made in most analyses of deuteron data to extract neutron information. The deuteron is more than the sum of its proton and neutron parts and since experiments on free neutrons can not be done, this nonadditive portion is important to evaluate by any means available. We believe, in fact, that earlier experiments [6,7] make it clear that the deuteron is the simplest nucleus exhibiting the EMC effect which, in turn, must affect the extraction of the neutron structure function that enters in these sum rules [8].

In the theoretical part of the present paper, we enlarge upon the work we introduced earlier [9] and apply it to some old data and to new, previously unpublished data. We have studied deep inelastic  $\nu$  and  $\bar{\nu}$  scattering from various targets, focusing on reactions that produce high momentum backward protons. Backward means relative to the incoming neutrino or antineutrino and high momentum means relative to kinematic limits upon backward momentum imposed in terms of quantities such as the target mass and momentum fraction carried by the struck quark.

We concluded, based on deuteron target data [10] obtained at CERN with  $\nu$  and  $\bar{\nu}$  beams, that the momen-

tum distribution of the backward protons was consistent with production from a multiquark component (6q) in the deuteron and was difficult to explain if produced via break-up of a two nucleon (2N) quantum mechanical state with a simple conventional wave function. The particular problem with the latter picture, where the neutron and proton substantially maintain their character as nucleons [11], was that there were more large momentum backward protons than expected from typical neutron-proton wave functions. However, in our previous work we were only able to calculate the shape of the backward proton spectrum in the two cases and not the absolute normalization or even the relative normalization of the 6q and 2N contributions.

In this paper, we will present normalized calculations for backward proton production in deep inelastic experiments for both the 2N and 6q deuteron components. The 6q calculation includes factors of the fraction of the deuteron that is 6q and of the fragmentation rate of the residue of the 6q cluster into protons. A numerical uncertainty in the latter rate for high momentum protons leads to a factor circa 2 uncertainty in fixing the fraction of 6q state in the deuteron; otherwise the calculation is well determined.

We denote the probability of finding the 6q configuration in the deuteron as  $f$ , with  $f$  expected to be between 0.01 and 0.07. Possible values for  $f$  have been calculated from deuteron wave functions as the probability for the nucleons to overlap, and Sato et al. [12] claim a value for  $f$  in the middle of this range for a typical nucleon-nucleon potential. The largest deuteron probability,  $f = 0.074$ , was used [13] in describing high energy SLAC electron-deuteron data at  $x > 1.0$ . Also, studies of the deuteron electromagnetic structure functions have been used to es-

timate  $f$  to be a few percent [14]. We here will find that the 6q contribution in deep inelastic scattering, even with  $f$  only one or two percent, can be quite large for energetic backward protons. Throughout, although we are mindful of many possibilities (see e.g., [15]), we simplify by speaking of the short range baryon number correlation as either 6q or 2N. Within this limitation, we can further say that for most of the conventional 2N wave functions, the 6q state not only can but also must contribute a major share of the cross section for energetic backward protons. We will show that at 500 MeV/c backward proton momentum the modern nucleon-nucleon potential that comes closest to our data needs at least a 60% additional contribution.

On the experimental side, we shall in the next Section discuss a Fermilab neutrino-deuteron 15-ft bubble chamber experiment (E545) which has obtained data (previously unpublished) on backward production of protons. Also, we shall comment on some published experiments which likewise measured high-momentum backward proton events.

In Sect. III, we give the theoretical formulae used in calculation of backward proton spectra to compare with the Fermilab and CERN deuteron break-up cross sections for backward protons. A comparison of the new data with previously published Argonne, Brookhaven, CERN, and Fermilab backward proton production data is also given. The comparisons of the prediction given by modern potentials with our data is in Sect. IV. The final Section is devoted to further discussion and presentation of conclusions.

## II. FERMILAB E545 NEUTRINO-DEUTERIUM DATA

Previous analyses of the E545 neutrino-deuteron data have concentrated on either extracting  $\nu n$  interaction data, or on the distributions of lepton or hadron variables in  $\nu d$  scattering. A typical analysis would separate the data into even-prong “ $\nu n$ ” and odd-prong “ $\nu p$ ” events, where a visible proton spectator is ignored in the prong count. The observed “ $\nu n$ ” events were assumed to be a sample of  $\nu n$  interactions depleted by “rescattering” within the deuteron nucleus. The “rescattered”  $\nu n$  events, in turn, would appear in the “ $\nu p$ ” event sample. In extraction of ratios of  $\nu n$  to  $\nu p$  cross sections the fraction of such rescattered events was estimated to be in the 6–12% range.

An excess of high momentum proton spectators, compared to standard deuteron wave function predictions, is known to be associated with the “ $\nu n$ ” event sample. When commented on in previous analyses, it would generally be noted that the origin of this excess is unknown, but given that the excess accounts for less than 1% of the “ $\nu n$ ” events any effect on the overall distributions or measured quantities would be negligible. In the present

analysis, we explicitly examine the  $\nu d$  target fragments in the E545 data, and compare the distribution of backward protons with a deuteron wave function plus a small six-quark component.

Many details of the E545 experiment have been published [16]. The data discussed here were previously presented at an APS meeting [17], where the emphasis was on establishing the existence of a “rescattering” phenomena which depleted the observed spectator proton (neutron target) event sample, and in estimating its frequency.

The E545 data are from a 320,000 frame exposure of the deuterium-filled Fermilab 15-ft bubble chamber to a wide-band single-horn focused neutrino beam produced by  $4.8 \times 10^{18}$  350 GeV/c protons incident on a beryllium oxide target. The anti-neutrino component of the beam is  $\approx 14\%$ . The film was scanned twice, and events with two or more charged tracks produced by incident neutral particles in a  $15.6 \text{ m}^3$  fiducial volume were accepted for analysis. All charged tracks were digitized and geometrically reconstructed. Topology-dependent weights are applied to the data to compensate for scanning and processing losses and for those events failing geometric reconstruction. The average processing times scanning efficiency is 0.80. Cuts are applied to the two-prong events to remove  $K^0$  and  $\Lambda$  decays and  $\gamma$  conversions from the data.

A kinematic technique which uses only the measured momenta of the charged particles is used to select a sample of charge current events. Only events for which  $\sum p_L > 5 \text{ GeV}/c$ , where  $p_L$  is the component of laboratory momentum in the beam direction and the sum is taken over all charged particles, are included in the analysis. The muon candidate is identified as that negative track in the event with the largest component of momentum transverse to the incident neutrino direction. Those events for which the component of the  $\mu^-$  candidate’s momentum transverse to the vector sum of the momenta of the other charged particles in the event is greater than  $1.0 \text{ GeV}/c$  are accepted as charge current events.

The incident neutrino energy of the selected charge current events is estimated using transverse momentum balance:  $E_\nu = p_L^\mu + p_L^H + |\vec{p}_T^\mu + \vec{p}_T^H| p_L^H / p_T^H$ , where the symbols  $p^\mu$  and  $p^H$  refer to the muon momentum and the vector sum of the charged hadron momenta, respectively. Only events with  $E_\nu > 10 \text{ GeV}$  are accepted for analysis.

A Monte Carlo simulation indicates that the sample selected according to the above criteria includes 79% of the  $\nu d$  charge current events, with the  $\mu^-$  correctly identified in 98% of the cases, and with a 3% contamination due to  $\nu d$  neutral-current events and 1% due to  $\bar{\nu} d$  events.

The corrected number of  $\nu d$  events in the sample is 15,129, with an average neutrino energy  $\langle E_\nu \rangle = 50 \text{ GeV}$ . Of these events, 459 have an identified proton with momentum magnitude greater than  $160 \text{ MeV}/c$  whose direction is backward with respect to the incident neutrino direction. (Significant visibility losses occur for protons with momentum less than  $160 \text{ MeV}/c$ , and hence are not presented.) The identity of the backward protons

was verified by re-examining all such tracks on the scan table. The momentum distribution of the backward protons is given in Table I. This data will be discussed in Sect. 3, together with the proton spectrum from a  $\nu d$  and  $\bar{\nu} d$  exposure of BEBC by the WA25 collaboration at CERN [10].

The published Fermilab E545 spectator proton spectra from quasi-elastic  $\nu d$  scattering ( $\nu d \rightarrow \mu^- pp_s$ ) [18] will also be discussed, together with similar distributions from  $\nu d$  bubble chamber experiments at Brookhaven (80-in) [19] and Argonne (12-ft) [20].

### III. THEORETICAL DISCUSSION

We will give the expressions for the charge current inclusive cross sections of neutrinos hitting a deuteron and producing a backward proton,  $p_B$ , a forward lepton,  $\ell^-$ , and anything else,  $X$ ,

$$\nu + d \rightarrow \ell^- + p_B + X, \quad (1)$$

in both the 2N and 6q models. We will see that the shape of the backward proton spectrum is different in the two cases, and will see if the calculations can match the data. The two contributions are not mutually exclusive, and we shall add them incoherently, weighting the 6q contribution by fraction  $f$  and the 2N contribution by  $(1 - f)$ . We expect that  $f$  will be on the order of a few percent, but that none-the-less the 6q contribution could be large at large backward proton momenta.

The fully differential cross section is differential in  $x$ ,  $y$ ,  $\alpha$ , and  $p_T$ , which are the experimentally measurable variables. These variables are the struck quark momentum fraction,

$$x = Q^2/2m_N\nu = Q^2/2m_N(E_\nu - E_\ell); \quad (2)$$

the fractional lepton energy loss,

$$y = \frac{E_\nu - E_\ell}{E_\nu}; \quad (3)$$

the light front momentum fraction of the backward proton,

$$0 \leq \alpha = \frac{E_p + p_z}{m_N} \leq 2 \quad (4)$$

(with  $p_z$  defined positive for backward protons); and the transverse momentum of the proton relative to the direction of the incident neutrino,  $p_T$ .

For the 2N model, using quark distribution functions appropriate to describe striking the neutron, with the argument changed from  $x$  to  $\xi = x/(2 - \alpha)$  because the neutron is moving, and having the proton emerge with probability given in terms of the deuteron wave function, we find the cross section

$$\begin{aligned} \frac{d\sigma_{2N}}{dx dy d\alpha d^2p_T} &= \sigma_0 \times \\ &\times (D_n(\xi) + S_n(\xi) + (1 - y)^2 \bar{U}_n(\xi)) \\ &\times \frac{(2 - \alpha)}{\gamma} |\psi(\alpha, p_T)|^2, \end{aligned} \quad (5)$$

where  $D_n(\xi)$  is  $\xi$  times the distribution function of down quarks in the neutron ( $n$ ), etc.,  $\gamma = E_p/m_N$ ,  $\sigma_0$  is the point Fermi weak interaction (with strength  $G_F$ ) cross section,

$$\sigma_0 \equiv \frac{2G_F^2 m_N E_\nu}{\pi}, \quad (6)$$

and  $\psi$  is the wave function of the deuteron normalized by

$$\int d\alpha d^2p_T |\psi(\alpha, p_T)|^2 = 1. \quad (7)$$

The corresponding cross section for the 6q component of the target can be written in terms of the probability distribution of a quark in the 6q cluster and in terms of the probability,  $D_{p/5q}$ , for the residuum of the 6q state to fragment into the proton. This time, since the deuteron or 6q cluster is stationary in the lab,  $x$  is directly—in the scaling limit—the momentum fraction of the struck quark. We have

$$\frac{d\sigma_{6q}}{dx dy d\alpha d^2p_T} = \sigma_0 D_6(x) \cdot \frac{1}{2 - x} D_{p/5q}(z, p_T), \quad (8)$$

where we have included just  $D_6$ , the down quark distribution for the 6q cluster times  $x$ , on the grounds that we will need the literal 5q residuum (which comes from the 6q Fock component of the nominal 6q cluster) to get the highest momenta backward protons. The first argument of the fragmentation function is the light front momentum fraction of the proton relative to the five quark residuum, or

$$z = \frac{\alpha}{2 - x}. \quad (9)$$

Momentum range (MeV/c)	Number of events
160-200	187
200-240	100
240-280	61
280-320	37
320-360	30
360-400	14
400-440	10
440-480	10
480-520	9
520-560	1
560-600	0

TABLE I. Momentum distribution of backward protons in 15,129  $\nu d$  charge current events from Fermilab experiment E545.

Presently reported data on the backward proton momentum spectrum uses protons gathered from the entire backward hemisphere. Hence, we too will integrate over the backward hemisphere, to allow direct comparison to experiment. We will integrate over  $x$  and  $y$  also. The term with explicit  $y$  dependence gives a small contribution. Then,

$$\begin{aligned} \frac{E_p}{p^2} \frac{d\sigma_{2N}}{dp} &= \int_{bkwd} d\Omega dx E_p \frac{d\sigma_{2N}}{d^3p dx} \\ &= \sigma_0 \bar{\xi}_{\nu n} \int_{bkwd} d\Omega dx \gamma^{-1} \alpha (2 - \alpha)^2 |\psi|^2 \end{aligned} \quad (10)$$

where

$$\bar{\xi}_{\nu n} = \int_0^1 d\xi \left( D_n(\xi) + S_n(\xi) + \frac{1}{3} \bar{U}_n(\xi) \right) \quad (11)$$

and

$$\begin{aligned} \frac{E_p}{p^2} \frac{d\sigma_{6q}}{dp} &= \int_{bkwd} d\Omega dx E_p \frac{d\sigma_{6q}}{d^3p dx} \\ &= \int_{bkwd} d\Omega dx \alpha D_6(x) D_{p/5q}(z, p_T), \end{aligned} \quad (12)$$

where  $p = |\vec{p}|$  is the backward proton momentum (and we used  $\alpha d\sigma/d\alpha d^2p_T = E d\sigma/d^3p$ ). What we want is the weighted sum of the 2N and 6q contributions,

$$\frac{d\sigma}{dp} = (1 - f) \frac{d\sigma_{2N}}{dp} + f \frac{d\sigma_{6q}}{dp}. \quad (13)$$

The plotted curves are based on the above formulas plus some choices for the deuteron wave function, the quark distribution functions, and the fragmentation function of the 5q residuum.

The wave function will be a light front wave function. (A simple use of a non-relativistic wave function conflicts with the kinematic bound on maximum backward proton momentum.) It is related to non-relativistic wave functions by

$$|\psi(\alpha, p_T)|^2 = |\psi_{LF}(\alpha, p_T)|^2 = \frac{E_k}{\alpha(2 - \alpha)} |\psi_{NR}(k_z, k_T)|^2 \quad (14)$$

where the arguments of the non-relativistic wave function are obtained from

$$k_T = p_T \quad (15)$$

and

$$\alpha = \frac{\sqrt{m_N^2 + \vec{k}^2} + k_z}{\sqrt{m_N^2 + \vec{k}^2}}. \quad (16)$$

The normalization is

$$\int d^3k |\psi_{NR}(k_z, k_T)|^2 = 1 \quad (17)$$

and the factor above comes from the Jacobian in

$$d^3k = \frac{E_k}{\alpha(2 - \alpha)} d\alpha d^2p_T. \quad (18)$$

We use several different deuteron wave functions, but start with a Hulthén wave function, which is still in common use [21,18,19],

$$\psi_{NR}(\vec{k}) \propto \frac{1}{\vec{k}^2 + (45.6 \text{ MeV})^2} - \frac{1}{\vec{k}^2 + (260 \text{ MeV})^2}. \quad (19)$$

The quark distributions for the nucleon are the set CTEQ1L [22]. (Some old and simple quark distributions [23] give results about the same.) For the 6q cluster, we use the Lassa-Sukhatme model “B” quark distributions [24]. These distributions are based on quark counting rules and physical logic and describe the EMC data. Models “A” and “C” are not very different for the present purposes and are omitted from the figures mainly to avoid clutter. Model “B” has

$$D_6(x) = 3 \times 1.85 \sqrt{\frac{x}{2}} \left(1 - \frac{x}{2}\right)^{10}. \quad (20)$$

The fragmentation function for the 5q residuum is taken in a factorized form,

$$D_{p/5q}(z, p_T) = \frac{(N+4)!}{N!3!} z^N (1-z)^3 \cdot \frac{2}{\pi \lambda^2} \left(1 + \frac{p_T^2}{\lambda^2}\right)^{-3}, \quad (21)$$

where  $\lambda = 310 \text{ MeV}$ . The spectrum of protons for  $z \rightarrow 1$  is given by the counting rules. For this limit, the two quarks not in the proton must give their momentum to the three that are, and this leads to the factor  $(1-z)^3$ . Then, barring effects external to the 5q residuum, the proton should have 3/5 of the residuum’s momentum and this requires  $N = 5$ . There is, however, some pull from the struck quark which could increase the probability of protons going in the forward direction. This can be accommodated in the above fragmentation function by reducing  $N$ , and we shall quote results for both  $N = 3$  and  $N = 5$ . Lower values of  $N$  increase the cited values of  $f$ .

Fig. 1 shows the comparison of the E545 data and WA25 data [10] with the sum of the 6q and 2N contributions, using  $N = 5$  and  $f = 2\%$ , or equivalently for  $N = 3$  and  $f = 4\%$ . The E545 data is absolutely normalized,  $d\sigma/dp = (\sigma_{tot}^{CC}(\nu d)/N_{tot}) N_{bin}/\Delta p$  where  $\Delta p$  is the bin width and  $\sigma_{tot}^{CC}(\nu d)$  is obtained from [25] and evaluated at the 50 GeV average  $E_\nu$  in the E545 experiment. The BEBC data WA25 is scaled to agree with the E545 data at the lower momenta.

The match between the calculation and the data is quite good. A 2N contribution alone, with this wave function, could not match the data. The 6q contribution,

though it is overall only 2–4% of the normalization of the deuteron state, contributes the major share of the cross section for energetic backward protons. The crossover momentum is about 300 MeV, and above this momentum a larger and larger majority of the protons come from the 6q cluster. To further elaborate this point, we note that at 500 MeV ( $c = 1$ ) backward proton momentum, the Hulthén contribution needs 800% additional contribution to be in agreement with the new data.

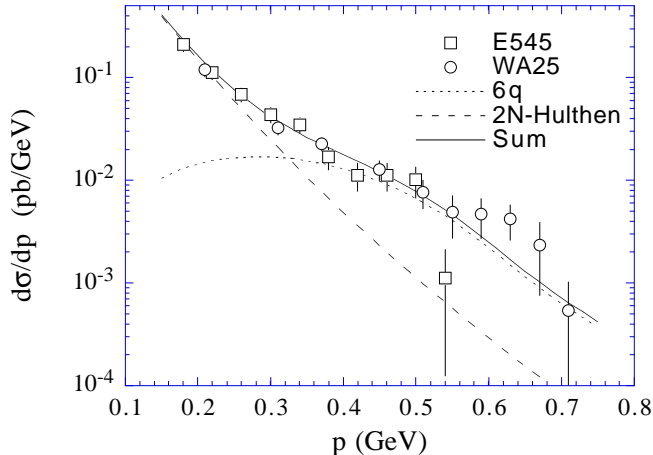


FIG. 1. Protons in backward hemisphere from neutrino induced deuteron breakup;  $p$  is the magnitude of the three momentum. The data is Fermilab 15-ft bubble chamber (E545) data and BEBC (WA25) data. The 6q curve as shown uses a fragmentation function whose transverse part has a power-law falloff,  $(1 + p_T^2/\lambda^2)^{-3}$ , and whose longitudinal part goes as  $z^5(1 - z)^3$ , and is normalized to give one proton per 6q cluster breakup. The normalization requires a 2% fraction of 6q state. Using instead  $z^3(1 - z)^3$  leads to a curve whose shape is essentially the same as the one shown in the important region above 250 MeV/c, and with the same normalization if the 6q fraction is 4%. The 2N calculation uses a Hulthén wave function [21], adjusted for use in a light front version of a relativistic calculation.

Backward proton data from neutrino scattering is also available from Argonne [20], Brookhaven [19], and again Fermilab E545 [18] for the “quasi-elastic” reaction,

$$\nu + d \rightarrow \mu^- + p + p_s, \quad (22)$$

where  $p_s$  is a label for the “slow protons” or “spectators.”

Fig. 2 shows the backward proton spectra from the three sets of “quasi-elastic” data, together with the spectra from the inelastic data of E545 and the WA25 data. There is reasonable consistency within errors among all the data sets for the proton spectrum, despite great differences in the incoming neutrino energy. One may think that the material struck by the incoming probe goes forward and that any backwardly emerging hadrons have spectra governed only by the distribution of constituents in the target. The consistency among the data sets for backward protons supports this view.

To repeat the main point of this section, a calculation modeling the deuteron as 2N plus a small amount of 6q is able to match the data out to about 720 MeV backward hemisphere proton momentum, again within experimental uncertainty.

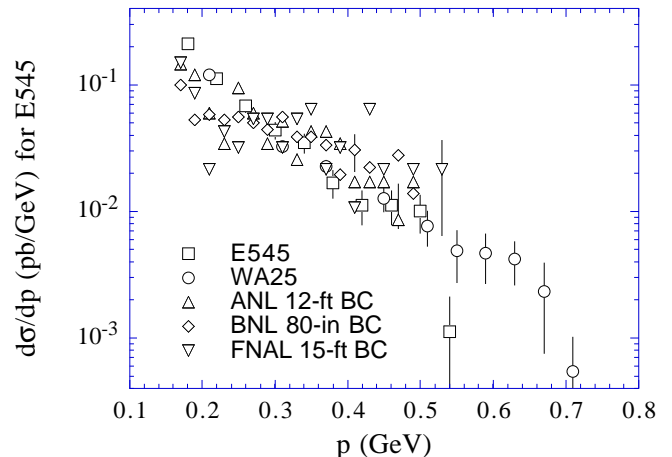


FIG. 2. Protons in the backward hemisphere from several different neutrino induced deuteron breakup experiments;  $p$  is the magnitude of the three momentum. The data labeled E545 and WA25 are for inclusive deuteron breakup, and the data labeled ANL, BNL, and FNAL (the latter actually also from E545) are for quasi-elastic deuteron scattering. The vertical scale is for the E545 inclusive data; the other data are scaled to it.

#### IV. USE OF OTHER WAVE FUNCTIONS

The two-nucleon wave function that we have used in the above discussion is fairly simple, and one may inquire what happens if a more realistic wave function is used. There are many wave functions derived from nucleon-nucleon potentials that are fit to nucleon-nucleon scattering data, and sometimes also to electron-deuteron scattering data. The assumption is made that only nucleon-nucleon, or sometimes only baryon-baryon, degrees of freedom are needed. If there are other degrees of freedom present—and that is a crucial question we are trying to address—they are ignored. But if they exist, their effects are present in nature, and they must be included in the fitted baryon-baryon potential. And if one calculates deuteron structure from such a potential, who is to be sure if small effects in the (high momentum) tail of the wave function are really due to the two nucleons, or due to the fitted wave function trying to emulate another degree of freedom? (We should quote the Paris group’s remark that “there is no compelling theoretical reason to believe the validity of our potential in the region  $r \leq 0.8$  fm. since the short range (SR) part of the interaction is related to exchange of heavier systems and/or to effects of subhadronic constituents such as quarks, gluons, etc.” [26] There apparently would be no physical

significance in the invention of a nucleon-nucleon potential model giving enhanced high momentum components by modifying this  $r \leq 0.8$  fm. region. But, the important point is: It is precisely this region that this our new data probes.)

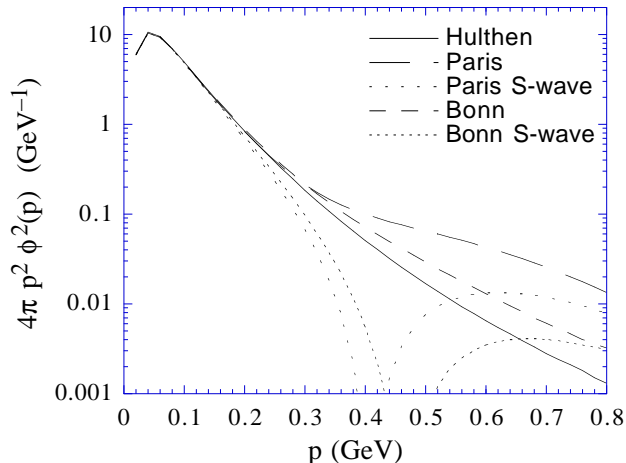


FIG. 3. Comparison of the Bonn, Hulthén, and Paris wave functions. (The  $\phi^2$  on the vertical axis is a sum of  $\phi_S^2$  and  $\phi_D^2$  for the Paris and Bonn wave functions.)

Thus, if one speaks of more realistic wave functions in the present context, one may object to the phrase “more realistic.” We shall however take the Paris and Bonn wave functions [27,28] as representative of more sophisticated wave functions and see what happens when we use them. A first plot, Fig. 3, shows the Paris, Bonn, and Hulthén wave function in momentum space. They are essentially the same at low momenta, but at several hundred MeV, thanks mainly to the shape and 5.77% size of the D-state, the Paris wave function is considerably larger. Among other wave functions, both the Reid wave function [29] and the relatively new wave function of Van Orden, Devine, and Gross [30] are rather close to the Paris wave function.

Fig. 4a shows what one of the Bonn wave functions, the energy independent OBEPQ [28] produces for the backward proton spectrum. Though a more complete and realistic wave function, the results are not strikingly different than those from the Hulthén wave function. Fig. 4b shows a corresponding plot for the Paris wave function. All these potential models of the nucleon-nucleon interaction give representations of our new data which are well below the data for the high momentum backward protons. At a momentum of 500 MeV ( $c = 1$ ), a considerable contribution must be added to each to bring them close to the data being presented: For the Hulthén, as noted above, the additional amount needed is 800%; for the Bonn model an increase of 350% is needed (see Fig. 4a) and for the Paris model, an additional 62% is needed to bring theory and experiment into agreement. The logarithmic scale for  $d\sigma/dp$  in these figures misleads the eye. But, in Fig. 4b, it is clear that the Paris curve

is below the majority of the data error bars. To make a more compelling statement, we give a simple statistical comparison of the Paris curves with our data in the momentum range,  $0.2 < p < 0.5$  GeV. The squares of the differences between the center of the data points and the dashed Paris and solid Paris + 6q curves divided by the error bar is calculated. The result is a value of  $\chi^2$  per data point of 0.8 for the solid curve and 3 for the dashed curve, corresponding to confidence levels of 0.5 and 0.003, respectively, where the Particle Data Groups, graphs are used as a most universal particle physics convention.

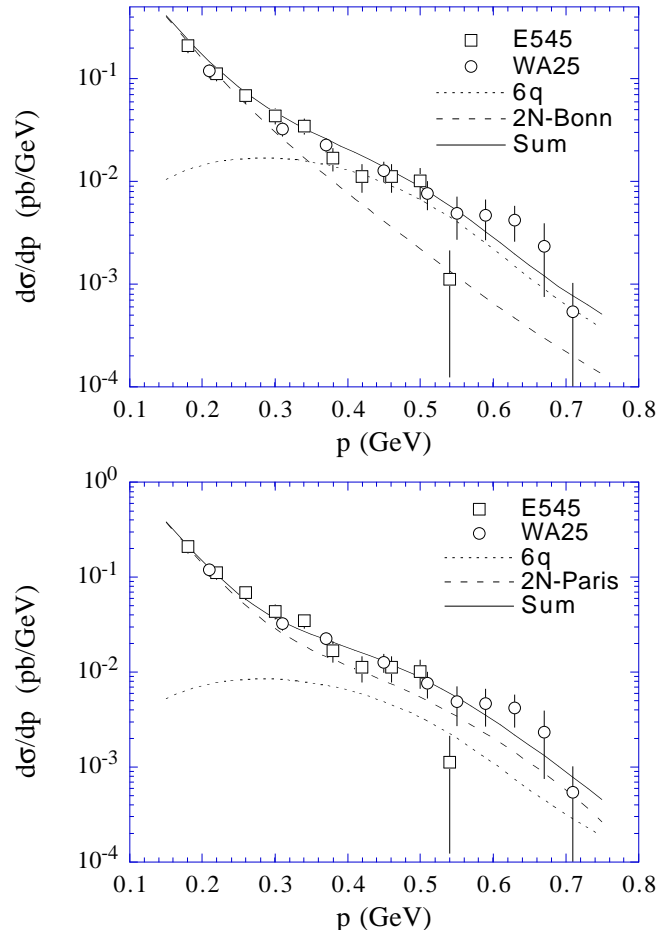


FIG. 4. Comparison of the backward proton spectrum in  $\nu + d \rightarrow \ell^- + p_B + X$  to calculations using the Bonn (energy independent OBEPQ) wave function and the Paris wave function, each using a  $z^5(1-z)^3$  form in the fragmentation function and with a 2% 6q contribution for the Bonn wave function case, 1% for the Paris case. As in Fig. 1, similar results follow with a  $z^3(1-z)^3$  form and a 4% or 2% 6q contribution for the respective cases.

## V. DISCUSSION AND CONCLUSIONS

We have seen that a small amount of 6q cluster in a deuteron can explain the backward proton data. It is still possible that some 2N wave function with an increased

amount of probability at high momenta could also explain the data. Therefore it is of interest to find other signatures that could signal the presence of the 2N or 6q states. We will mention two possibilities, one if a polarized deuteron target is available, another if there is enough data to bin in both  $x$  and  $p$ , and then conclude.

If a polarized target is available, then the 2N model leads to characteristic variations of the backward proton angular distribution. At low momentum, the wave function is mostly S-wave and the backward distribution is angle independent regardless of the deuteron's polarization. At a momentum where the D-state dominates (about 400 MeV for the Paris wave function, as in Fig. 3), a polarized deuteron has a non-isotropic spatial wave function. Fig. 5 shows the angular distribution of backward protons from the D-state for both a longitudinally polarized deuteron (i.e.,  $J_z = 0$  with quantization direction along the incoming current) and for the average of the two transverse polarizations. (The latter would be for either transverse polarization in the analogous electromagnetic case.)

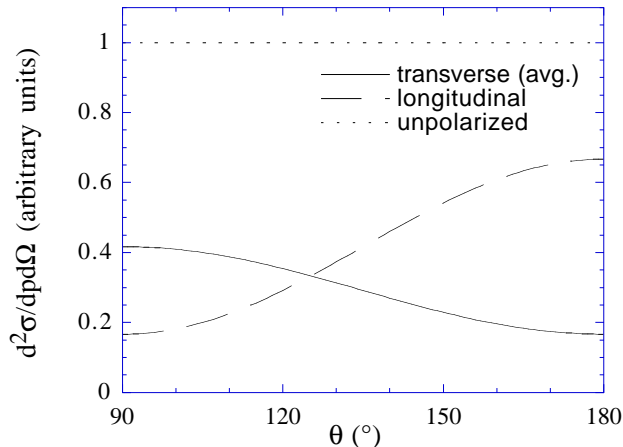


FIG. 5. Angular distribution of backward protons assuming a polarized deuteron, the 2N model, and a momentum at which the D-state dominates. The solid curve is for the average over the two transverse polarizations of the deuteron, the dashed curve is for the longitudinal polarization, and the dotted line shows the sum over all polarizations.

If we can bin data in both  $x$  and  $p$ , then we can define a “two-nucleon test ratio.” This is simply the ratio of the observed differential cross section for backward proton scattering to the cross section for scattering off a neutron with an appropriate momentum shift. The latter is intended to be just what would be expected for the 2N model, with the wave function factor removed. Explicitly,

$$R_1 = \frac{\sigma_{meas}(x, y, \alpha, p_T)}{\sigma_{nX}(x, y, \alpha, p_T)}, \quad (23)$$

where the denominator is

$$\sigma_{nX} = \frac{d\sigma}{dx dy}(\nu n \rightarrow \mu^- X)$$

$$= K(2 - \alpha) [D_n(\xi) + S_n(\xi) + (1 - y)^2 \bar{U}_n(\xi)]. \quad (24)$$

If the 2N model is correct, then

$$R_1 = |\psi(\alpha, p_T)|^2. \quad (25)$$

Thus, we can test for the 2N model by plotting  $R_1$  vs.  $x$  at fixed  $\alpha$  and  $p_T$ , or at fixed  $p$ . If the 2N model is right, such a plot would produce just a simple horizontal line. The crucial question is how different a result a 6q cluster would give. We have elaborated on this question in Ref. [31] for the electromagnetic case. If the 6q cluster dominates at some fixed backward proton momentum, it gives a curve for  $R_1$  vs.  $x$  that varies by a factor of roughly two from peak to valley. It should be easily distinguishable from the 2N expectation.

In conclusion, we have studied the production of backward protons in neutrino- and antineutrino-deuteron scattering, and compared the existing data to one model. The backward proton data from the E545 Fermilab experiment shown in this paper has not previously been published, although it has appeared in talks [17]. The model we have considered is an incoherent sum of contributions from 2N and 6q components of the deuteron. None of the 2N models that we have looked at has by itself a large enough high momentum tail to explain the backward proton data above about 300 MeV/c. If we add a 6q component, we get straightforwardly a good match to the shape of the backward proton spectrum at high momentum. If the probability of the 6q cluster is one to a few percent in the deuteron, then the 6q contribution accounts well for the observed normalization of the data at high momentum, while adding negligibly to the 2N contribution below about 250 MeV/c [32].

We consider this a good indication that 6q configurations exist in the deuteron and can be observed in certain circumstances. It is however not ironclad proof since in principle it may be possible that some 2N wave function with an enhanced high momentum tail could also explain all the backward proton data. But one should realize that a wave function gotten from a potential that is fit to data, including low energy nucleon-nucleon scattering data, is matching a Nature that may contain 6q cluster effects and must mock them up somehow in the context of its own degrees of freedom. This means that a good fit to the data with just a 2N wave function is not in its own turn ironclad proof against a 6q cluster. Hence we have added suggestions of further tests that may eventually argue directly against the 2N models.

## ACKNOWLEDGMENTS

We express our appreciation to the Fermilab E545 collaboration for providing their unpublished  $\nu d$  backward proton spectrum. CEC thanks the NSF for support under Grant PHY-9600415, and also O. Benhar, S. Liuti, and V. Nikolaev for useful comments. CEC and KEL

both thank Fermilab for its hospitality while part of this work was done.

- 
- [1] J. Ashman *et al.*, Nucl. Phys. B **328**, 1 (1989); Phys. Lett. B **206**, 364 (1988).
  - [2] G. Baum *et al.*, Phys. Rev. Lett. **51**, 1135 (1983); M.J. Alguard *et al.*, Phys. Rev. Lett. **37**, 1261 (1978); see also G. Igo and V. W. Hughes, Proceedings of the Vancouver Meeting-Particles and Fields '91, Eds. D. Axen, D. Bryman, and M. Comyn (World Scientific, Singapore, 1992) p. 593.
  - [3] P. Amaudruz *et al.*, Phys. Rev. Lett. **66**, 2712 (1991).
  - [4] B. Adeva *et al.*, Phys. Lett. B **302**, 533 (1993).
  - [5] P.L. Anthony *et al.*, Phys. Rev. Lett. **71**, 959 (1993).
  - [6] J.J. Aubert *et al.*, Phys. Lett. **123B**, 275 (1983).
  - [7] R. Arnold *et al.*, Phys. Rev. Lett. **52**, 727 (1984).
  - [8] K. E. Lassila, C. E. Carlson, A. Petridis, and U. P. Sukhatme, in Proceedings of XIV International Kazimierz Conference, Warsaw, 1991, ed. by Z. Ajduk, S. Pokorski, and A. Wróblewski (World Scientific, Singapore, 1992) p. 579.
  - [9] C.E. Carlson, K.E. Lassila, and U.P. Sukhatme, Phys. Lett. B **263**, 277 (1991).
  - [10] Quoted in E. Matsinos *et al.*, Z. Phys. C **44**, 79 (1989).
  - [11] L.L. Frankfurt and M.I. Strikman, Phys. Lett. B **69**, 93 (1977).
  - [12] M. Sato, S. Coon, H. Pirner, and J. Vary, Phys. Rev. C **33**, 1062 (1986).
  - [13] G. Yen and J. Vary, Phys. Rev. C **40**, R16 (1989).
  - [14] A. Kobushkin, Yad. Fiz. **28**, 495 (1979) [Translation, Sov. J. Nucl. Phys. **28**, 252 (1978)].
  - [15] N. S. Manton, Phys. Rev. Lett. **60**, 1916 (1988); E. Braaten and L. Carson, Phys. Rev. D **38**, 3525 (1988); R. A. Leese, N. S. Manton, and B. J. Schroers, Report "Attractive Channel Skyrmions and the Deuteron," DTP 94-47, NI 94037, hep-ph/9502405 (1995);
  - [16] see, e. g., J. B. Cole *et al.*, Phys. Rev. D **37**, 1105 (1988) and references therein.
  - [17] T. Kafka *et al.*, Bull. Am. Phys. Soc. **28**, 756 (1983) (E545 collaboration).
  - [18] T. Kitagaki *et al.*, Phys. Rev. D **28**, 436 (1983).
  - [19] N. J. Baker *et al.*, Phys. Rev. D **23**, 2499 (1981); T. Kitagaki *et al.*, Phys. Rev. D **42**, 1331 (1990).
  - [20] S.J. Barish *et al.*, Phys. Rev. D **16**, 3103 (1977).
  - [21] A. G. Tenner, Deuteron properties studied in neutrino and antineutrino interactions, NIKHEF-H/86-7; L. Hulthén, Ark. Mat. Fys. **28**, 5 (1942).
  - [22] J. Botts *et al.*, Phys. Lett. B **304**, 159 (1993).
  - [23] C.E. Carlson and T.J. Havens, Phys. Rev. Lett. **51**, 261 (1983).
  - [24] K.E. Lassila and U.P. Sukhatme, Phys. Lett. B **209**, 343 (1988).
  - [25] T. Kitagaki *et al.*, Phys. Rev. Lett. **49**, 28 (1982).
  - [26] M. Lacombe *et al.*, Phys. Rev. C **21** 861 (1980).
  - [27] M. Lacombe *et al.*, Physics Letters B **101** 139 (1981).
  - [28] R. Machleidt *et al.*, Phys. Rep. **149**, 1 (1987).
  - [29] R.V. Reid, Ann. Phys. (N. Y.) **50**, 411 (1968).
  - [30] J. W. Van Orden, N. Devine, and F. Gross, Phys. Rev. Lett. **75**, 4369 (1995).
  - [31] C. E. Carlson and K. E. Lassila, Phys. Rev. C **51**, 364 (1995).
  - [32] There may also be effects for fast forward protons; see S. Simula, Few Body Syst. Supp. **9**, 466 1995 and C. Ciofi degli Atti and S. Simula, Phys. Lett. B **325**, 276 (1994).